

## Article

# Enhancing the Tribo-Mechanical Performance of LDPE Nanocomposites Utilizing Low Loading Fraction Al<sub>2</sub>O<sub>3</sub>/SiC Hybrid Nanostructured Oxide Fillers

Ibrahim A. Alnaser <sup>1,2</sup>, Ahmed Fouly <sup>1</sup>, Muhammad Omer Aijaz <sup>2</sup>, Jabair A. Mohammed <sup>2</sup>,  
Mahmoud B. Elsheniti <sup>1</sup>, Sameh A. Ragab <sup>2</sup> and Hany S. Abdo <sup>2,\*</sup>

<sup>1</sup> Mechanical Engineering Department, Collage of Engineering, King Saud University, Riyadh 11421, Saudi Arabia; ianaser@ksu.edu.sa (I.A.A.); amohammed7.c@ksu.edu.sa (A.F.); mbadawy.c@ksu.edu.sa (M.B.E.)

<sup>2</sup> Center of Excellence for Research in Engineering Materials (CEREM), Deanship of Scientific Research, King Saud University, Riyadh 11421, Saudi Arabia; maijaz@ksu.edu.sa (M.O.A.); jmohammed@ksu.edu.sa (J.A.M.); sragab@ksu.edu.sa (S.A.R.)

\* Correspondence: habdo@ksu.edu.sa

**Abstract:** This research work highlights the tribomechanical investigations of using a low loading fraction of two ceramics combinations, Alumina (Al<sub>2</sub>O<sub>3</sub>) and Silicon Carbide (SiC) as reinforcement for Low-density Polyethylene (LDPE) matrix. The hybrid additives with different weight percentages (0.1 + 0.1, 0.25 + 0.25 and 0.5 + 0.5 wt%) were mixed with LDPE matrix and the degree of homogeneity was controlled using double-screw extruder prior to fabricating the composite samples via the injection molding machine. The nanoparticles fillers were characterized by field emission scanning electron microscope (FESEM), EDX and particle size analyzer to check its morphology, composition and size distribution. Thermogravimetric analyzer (TGA) and melting flow index (MFI) were performed for the fabricated nanocomposites samples. The mechanical properties of the nanocomposite were evaluated by performing tensile test, bending test and Shore-D hardness test, while the tribological performance was investigated using a ball on disk apparatus under different applied loads and sliding times. Moreover, in order to confirm the load-carrying capability of the composite, contact stresses was measured via finite element model using ANSYS software. The results show that the incorporation of low fraction hybrid ceramic nanoparticles can contributed positively in the tribological and mechanical properties. Based on the experimental results, the maximum improvement in the tensile strength was 5.38%, and 8.15% for hardness LDPE with 0.5 Al<sub>2</sub>O<sub>3</sub> and 0.5 SiC, while the lowest coefficient of friction was noticed under normal load of 10 N, which was approximately 12.5% for the same composition. The novel approach of incorporating low fraction hybrid ceramic nanoparticles as reinforcement for LDPE matrix is investigated, highlighting their positive contributions to the tribological and mechanical properties of the resulting nanocomposites.

**Keywords:** tribo-mechanical behavior; LDPE; hybrid nanocomposites; Al<sub>2</sub>O<sub>3</sub>-SiC; finite elements



**Citation:** Alnaser, I.A.; Fouly, A.; Aijaz, M.O.; Mohammed, J.A.; Elsheniti, M.B.; Ragab, S.A.; Abdo, H.S. Enhancing the Tribo-Mechanical Performance of LDPE Nanocomposites Utilizing Low Loading Fraction Al<sub>2</sub>O<sub>3</sub>/SiC Hybrid Nanostructured Oxide Fillers. *Inorganics* **2023**, *11*, 354. <https://doi.org/10.3390/inorganics11090354>

Academic Editor: Kenneth J.D. MacKenzie

Received: 25 July 2023

Revised: 23 August 2023

Accepted: 27 August 2023

Published: 29 August 2023



**Copyright:** © 2023 by the authors. Licensee MDPI, Basel, Switzerland. This article is an open access article distributed under the terms and conditions of the Creative Commons Attribution (CC BY) license (<https://creativecommons.org/licenses/by/4.0/>).

## 1. Introduction

There has been an increase in interest in using nanostructured oxide fillers as reinforcements for different materials and polymers in recent years. These nanostructured oxide fillers, such as Al<sub>2</sub>O<sub>3</sub> and SiC, have unique nanoscale characteristics that can improve the mechanical and tribological performance of the host materials. These fillers' high surface area-to-volume ratio and customized surface chemistry enable better interfacial interactions and load transmission inside the composite matrix [1,2].

Polyolefin-based low-density polyethylene (LDPE) is produced in considerable quantities for a variety of commercial items, including pipes [3], shielding [4], food packaging [5] and electrical insulation [6] because of its strength. LDPE can be shaped into a variety of

applications because of its structural strength and impact resistance, lightweight, high flexibility, low processing cost, moisture resistance and superior mechanical quality. Since LDPE products do not contain BPA (bisphenol A), their use is expected to increase as consumers become more aware of the dangers BPA poses to their health. Therefore, market players are focusing on enhancing LDPE manufacturing processes in order to develop high mechanical strength LDPE-based products. Recently, many attempts have been made to improve the mechanical properties of LDPE by blending it with different inorganic/organic nanofillers such as aluminum oxide ( $\text{Al}_2\text{O}_3$ ) [7,8], zinc oxide (ZnO), titanium oxide ( $\text{TiO}_2$ ), clay, silicon carbide (SiC) and carbon nanotubes (CNT). Adding a small amount of these nanofillers offered a better performance of LDPE composites in automotive, aerospace, construction and electronic application by improving physical and mechanical, anticorrosion and flame retardancy properties [9–12]. Several studies have been conducted in the recent decade to investigate the role of nanoparticles in tribological polymer nanocomposites [13–16]. According to these studies, the ideal nanoparticle concentration ranges for mechanical and wear properties are generally low, often ranging from 0.5 to 5 vol-%. [17–19]. Agglomeration is expected to occur after a particular percentage of nanoparticle loading, defining the maximum loading of addition [20]. Jani et al. [19] successfully improved the sliding wear behavior of PE-based polymer using a small number of silica and graphene oxide nanofillers. The addition of 0.5 wt% of vinyl silane-treated fumed silica achieved an 80% reduction in the specific wear rate compared to neat polymer. Sergey et al. [11] established a design to investigate the tribological characteristics of ultrahigh molecular weight polyethylene (UHMWPE)-carbon nanofiber composites. The 0.5 wt.% carbon nanofibers loading was determined to be the most effective filler under moderate tribological loading conditions. Noorunnisa et al. [20] revealed that maximum 4 wt.% alumina powder-filled composites had the best tensile strength and tensile modulus when compared to recycled LDPE, which improved by 34.88 and 91.57%, respectively.

Adding alumina to LDPE enhances various properties such as thermal, physical and mechanical properties along with crystallinity changes. Research by Deepak et al. [21] has found that this reinforcing filler brings about positive effects on the composite matrix. An increase in the modulus of elasticity, tensile strength and thermal stability have been observed. Similarly, the introduction of alumina fillers in the composite increased the packing efficiency that caused a reduction in the amorphous region, improved the interfacial interaction between LDPE and alumina filler and promoted an increase in the crystallinity of the polymer.

Ceramic nanoparticles with low porosity provide better mechanical characteristics such as good compressive strength [22], hardness [23] and low density [24]. SiC and  $\text{Al}_2\text{O}_3$  are popular reinforcing additives in the market due to their demand in the electrical, electronics, automotive and related industries. They are effective in improving the tensile strength and hardness of polymers, making them suitable for enhancing material properties. As a result, they hold a significant volumetric proportion of the global market for reinforcing additives. [25,26]. Alumina is a commonly used ceramic due to its low cost, easy processing and diverse applications. However, its low toughness and fracture energy can limit its use. The addition of SiC has shown improved results in strengthening the polymeric matrix. [26]. By adding SiC to the matrix, its modulus of elasticity was increased which resulted in increased flexural strength, greater hardness and higher fracture toughness [27,28]. A composite material comprising a thermoplastic polymer and alumina can address the drawback of low fracture toughness exhibited by ceramics. This approach has the potential to enhance the mechanical properties of the polymeric composite, making them more resilient to cracking and fracture. The addition of the ceramic nanoparticles, forming a composite, offers a viable solution to improve the strength and durability of the neat polymer, expanding their range of applications across a wide variety of industries. The development of stronger alternatives to LDPE products is crucial for a sustainable future. Additionally, the use of crosslinking agents or reactive extrusion processes can produce an improved LDPE product with high mechanical, friction strength and wear rate. Wear rates

and friction coefficients are usually included in tribology. SiC and Al<sub>2</sub>O<sub>3</sub> NPs exhibit good mechanical and wear resistance properties. However, there has not been not much research conducted on the tribological and surface characteristics of LDPE composites reinforced with Al<sub>2</sub>O<sub>3</sub> and SiC particles.

This work offers a study of LDPE nanocomposite reinforced with Al<sub>2</sub>O<sub>3</sub> and SiC hybrid nanoparticles and evaluates the mechanical, and tribological characteristics of developed composites for usage as lightweight engineering products. The selection of LDPE matrix composites was based on their ability to mitigate toughness and abrasion strength issues since ceramic materials are brittle.

## 2. Experimental Procedure

### 2.1. Materials

In this study, Low Density Polyethylene (LDPE) from TASNEE LD (grade 0725N), Saudi Arabia with Melt Flow Rate of 0.75 g/10 min was selected as a base polymeric matrix. Aluminum Oxide Al<sub>2</sub>O<sub>3</sub> powder with particle size less than 150 nm from Sigma–Aldrich (Burlington, MA, USA) and Silicon Carbide SiC powder with particle size less than 100 nm from Sigma–Aldrich (Burlington, MA, USA) were used as a hybrid nanofillers.

### 2.2. Samples Preparation

The premixing of LDPE with the two types of nano-powders of an equal weight percentage of (0.1 + 0.1, 0.25 + 0.25 and 0.5 + 0.5 wt%) to represent a total amount of 0.2, 0.5 and 1 wt% from nanofillers hybrid additives were performed at room temperature using 400 rpm mixer (variable speed mechanical mixer from Cole-Parmer, USA) for 10 min in order to distribute the hybrid nanopowders around the LDPE pellets homogeneously. As shown in the Figure 1, the mixtures were then extruded using a twin-screw extruder (Model LHFD1-130718) by Lab Tech Engineering Company, Limited (Mueang Samut Prakan District, Thailand) with ten heating zones starting by 160 °C and ending by 210 °C at the extruder nozzle. The speed of the screws during the extrusion process was adjusted to 40 rpm for two extrusion shots in order to obtain a very homogeneous composition which feed directly the pelletizer section (Model LZ-80) by Lab Tech Engineering Company, Limited (Mueang Samut Prakan District, Thailand) to get uniform pellets. Last step is feeding these pellets into the injection molding machine (Model JM138-Ai-SVP/2) by Chen Hsong (Hong Kong) in order to fabricate the final nanocomposite sets of samples needs for different characterizations and testing (Figure 2). The barrel temperatures of the injection nozzle have four different zones of 185, 190, 210 and 225 °C at the tip, and inject time of 1.4 s.

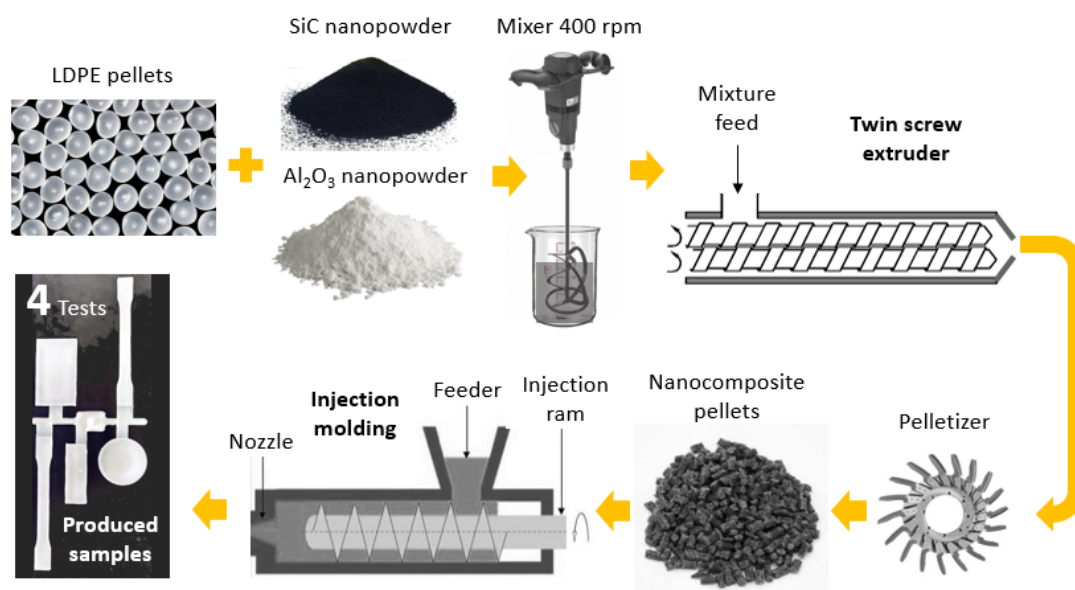
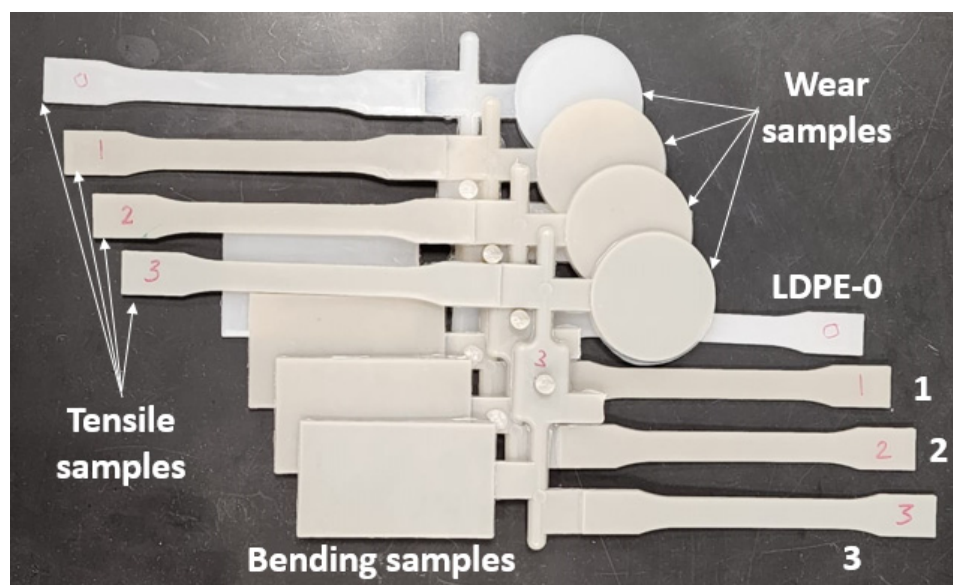


Figure 1. Schematic for the nanocomposite samples preparation steps.



**Figure 2.** Picture of the fabricated samples (Pure LDPE and three different composites).

### 2.3. Characterization and Testing

The characterization of the nanofillers were carried out using field emission scanning electron microscope FE-SEM, model: JEOL JSM-7600F, Tokyo, Japan, with Oxford EDX accessory attached to it, while the particle size distribution was analyzed using NKT-N9 laser particle size analyzer. The melting flow index (MFI) was obtained using ST-400A Melt flow index tester from China according to (ASTM) standard D1238 [29]. The test was performed at temperature of 230 °C and weight of 5 kg.

On LDPE-based composites, thermogravimetric analysis (TGA) was carried out utilizing a TGA-Q600 machine from TA Instrument, New Castle, DE, USA. The samples were put in an alumina pan, and thermal analysis was carried out in a nitrogen (N<sub>2</sub>) environment from 25 to 600 °C at a rate of 10 °C/min. Onset temperature, peak degradation temperature and final degradation temperature of the composite samples were recorded.

A Shore-D hardness test was performed on the fabricated nanocomposite according to ASTM D2240-15 standard [30] using a durometer. The readings were recorded after one second from touching the sample surface by the durometer needle. Six to ten measurements were taken for each sample and the average was calculated.

Bending or Flexural tests were performed according to ASTM D790 standard [31] using INSTRON testing machine model 3385H, Germany at a crosshead speed of 2 mm/min. The three-point mechanism was adjusted to 50 mm distance for the support span (L), and 5 samples per each composition were tested.

The tensile test was performed according to ASTM D638-14 standard with type I sample [32] using tensile testing machine of 150 kN, from INSTRON 3385H, Germany at a crosshead speed of 2 mm/min. The dimensions of the tensile test specimen are shown in Figure 3, where  $l_3 = 165$ ,  $l_2 = 115$ ,  $l_1 = 70$ ,  $L_0 = 60$ ,  $L = 120$ ,  $r = 75$ ,  $h = 3$ ,  $b_1 = 12$  and  $b_2 = 18$  mm. Five test replicates were performed for each composite to get the average value.

The tribology test was performed using Bruker CETR Tribometer (UNMT-1L) with ball on disk arrangement. The nanocomposite sample is representing by the rotating disk of 100 rpm rotational speed, while the ball is from chrome steel (E52100, HRC 63) with 10 mm diameter. The tribology test was performed according to ASTM G99-95 standard [33] under dry sliding conditions at room temperature. During wear test, 10 N, 30 N and 50 N loads were applied for time intervals of 5, 10, 15 and 20 min. To evaluate the load-carrying capacity of LDPE/Al<sub>2</sub>O<sub>3</sub>/SiC composites, it is essential to analyze the distribution of contact stresses and measure the stress on contact during the process. This is necessary to confirm the load-carrying capability of the materials concerning the applied load via finite

element model using ANSYS software. By measuring the contact stresses, it is possible to determine the load-carrying capacity of the composites, thus ensuring their suitability for specific applications.

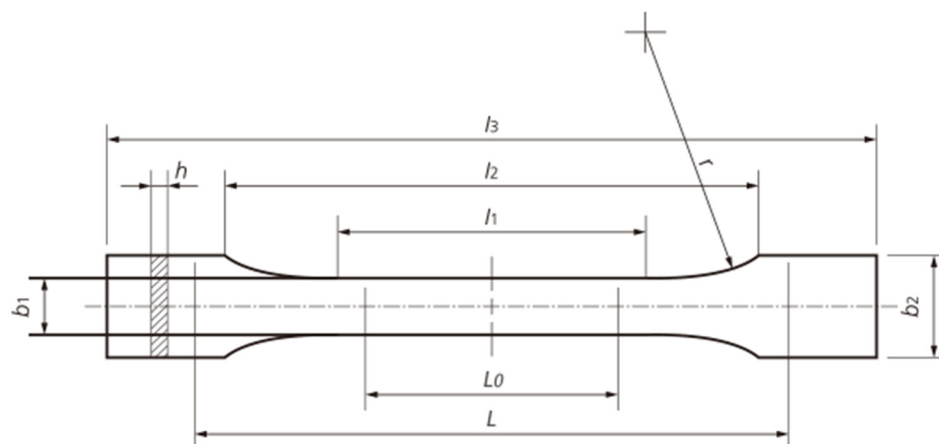


**Figure 3.** Tensile sample dimensions according to ASTM D638 standard.

### 3. Results and Discussion

#### 3.1. Nanostructured Oxide Fillers Characterization

Figure 4a,b show the SEM micrographs of  $\text{Al}_2\text{O}_3$  and SiC nanoparticles. As can be noticed, a spherical shape with a mean particle size ranged between 100–150 nm and 25–100 nm, respectively, is clearly presented, which also confirmed using particle size analyzer, and the size distribution is presented in Figure 4e,f. The chemical composition of the nanostructured oxide fillers was investigated using Energy-Dispersive X-ray Spectroscopy (EDX). The results show that the  $\text{Al}_2\text{O}_3$  consists of 37.10 wt.% Aluminum, 56.10 wt.% Oxygen and 6.8 wt.% Pt. While the SiC consists of 56.89 wt.% Carbon, 35.01 Silicon and 8.1 wt.% Platinum. The platinum in the EDS pattern is the result of a platinum coating applied to the sample prior to imaging. This coating enhances the surface conductivity of the sample, minimizing the charging impact and allowing for clear SEM pictures with no charge spots.

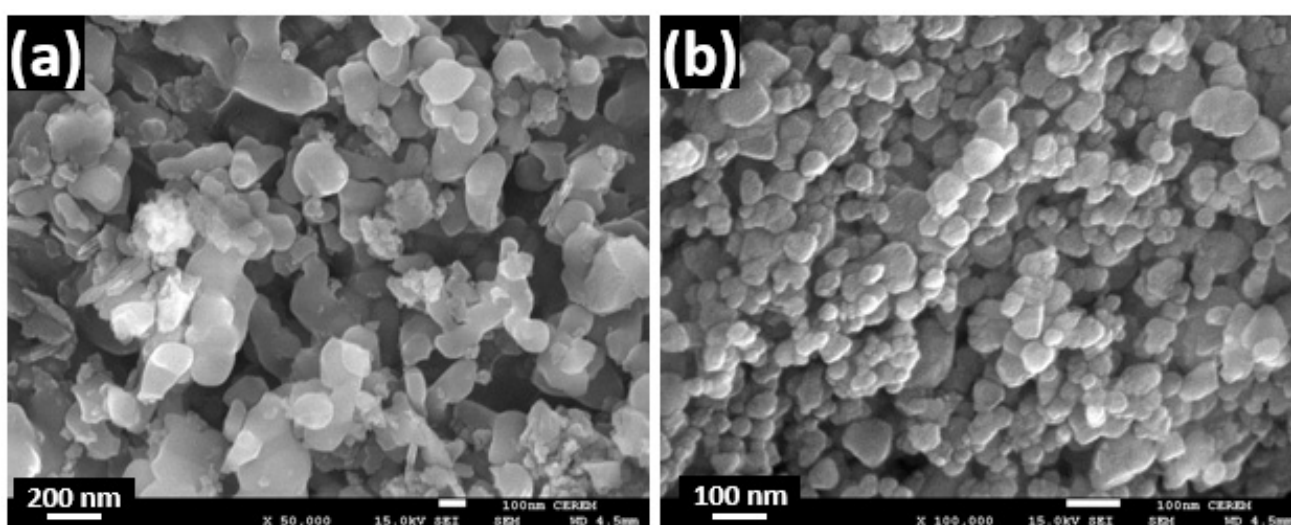


**Figure 4.** Cont.

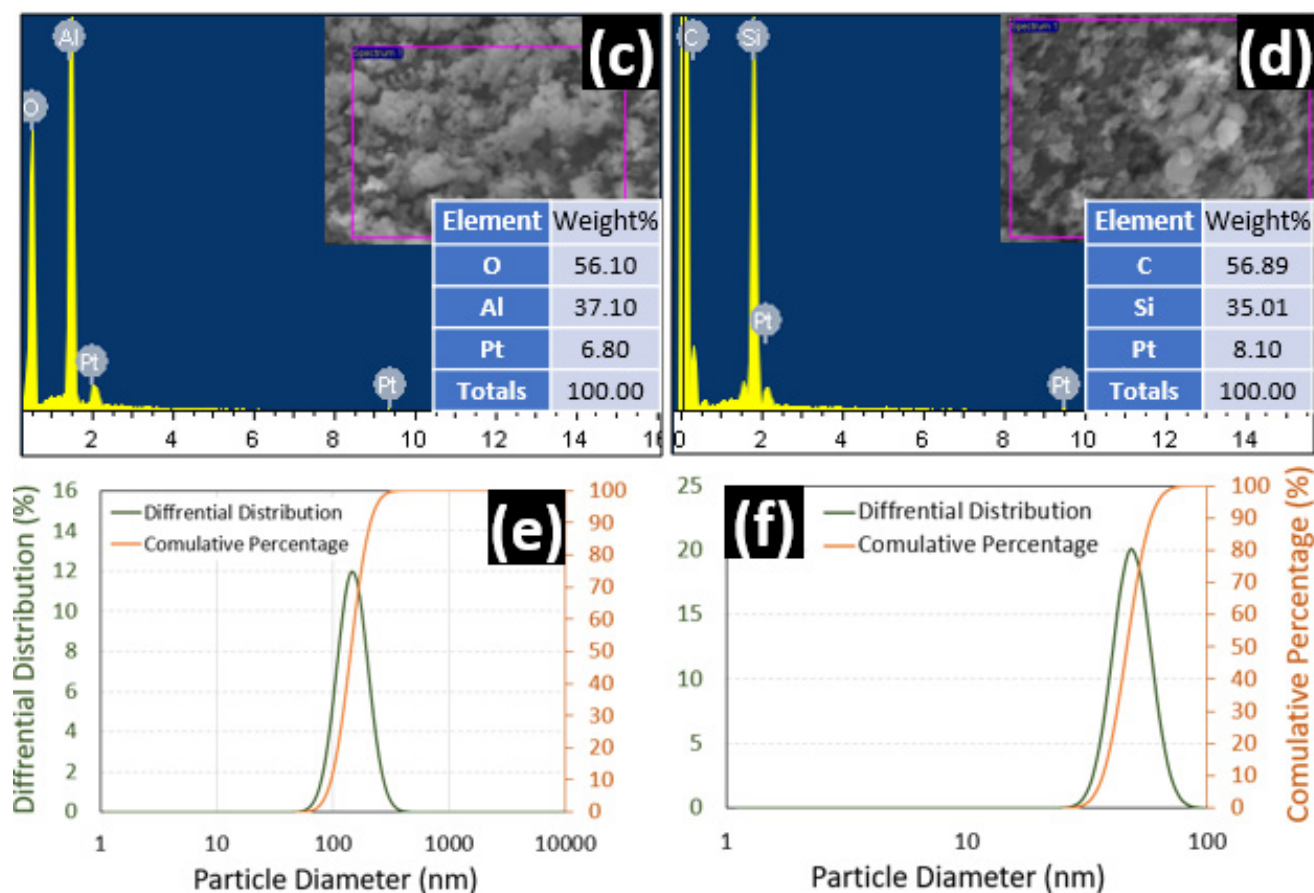


**Figure 4.** SEM images for the (a) Al<sub>2</sub>O<sub>3</sub> nanoparticles, (b) SiC nanoparticles, (c) EDX analysis for Al<sub>2</sub>O<sub>3</sub>, (d) EDX analysis for SiC, (e) particle size distribution for Al<sub>2</sub>O<sub>3</sub> and (f) particle size distribution for SiC.

### 3.2. Nanocomposite Characterization

Based on Figure 5, it appears that the mapping analysis includes elemental analysis to demonstrate the distribution of each element. This analysis helps determine if the additives are evenly distributed within the base matrix. The distribution of all elements observed in the mapping analysis confirms that the additives are indeed evenly distributed within the base matrix.

Table 1 shows the samples designation codes with the selected compositions in weight percent. While Figure 6 and Table 1 shows the thermal characteristics of virgin LDPE and its composites. All of the samples exhibit a single degradation process. The onset and peak degradation temperature of the composite and pure LDPE were identical. This could be due to the small additive quantities; however, in the final degradation, temperature for composite LDPE showed delayed degradation when compared to pure LDPE. The thermal stability of LDPE is improved by the high proportion of Al<sub>2</sub>O<sub>3</sub> and SiC. These thermal data show that small additions of additives reduce chain motion and thermal vibration and prevent the complete thermal deterioration of LDPE by acting as an effective thermal stabilizer. Other experiments with similar findings indicated no changes in initial degradation temperature but raised final degradation temperatures of the polymer composite with minor additions of additives [20,34].

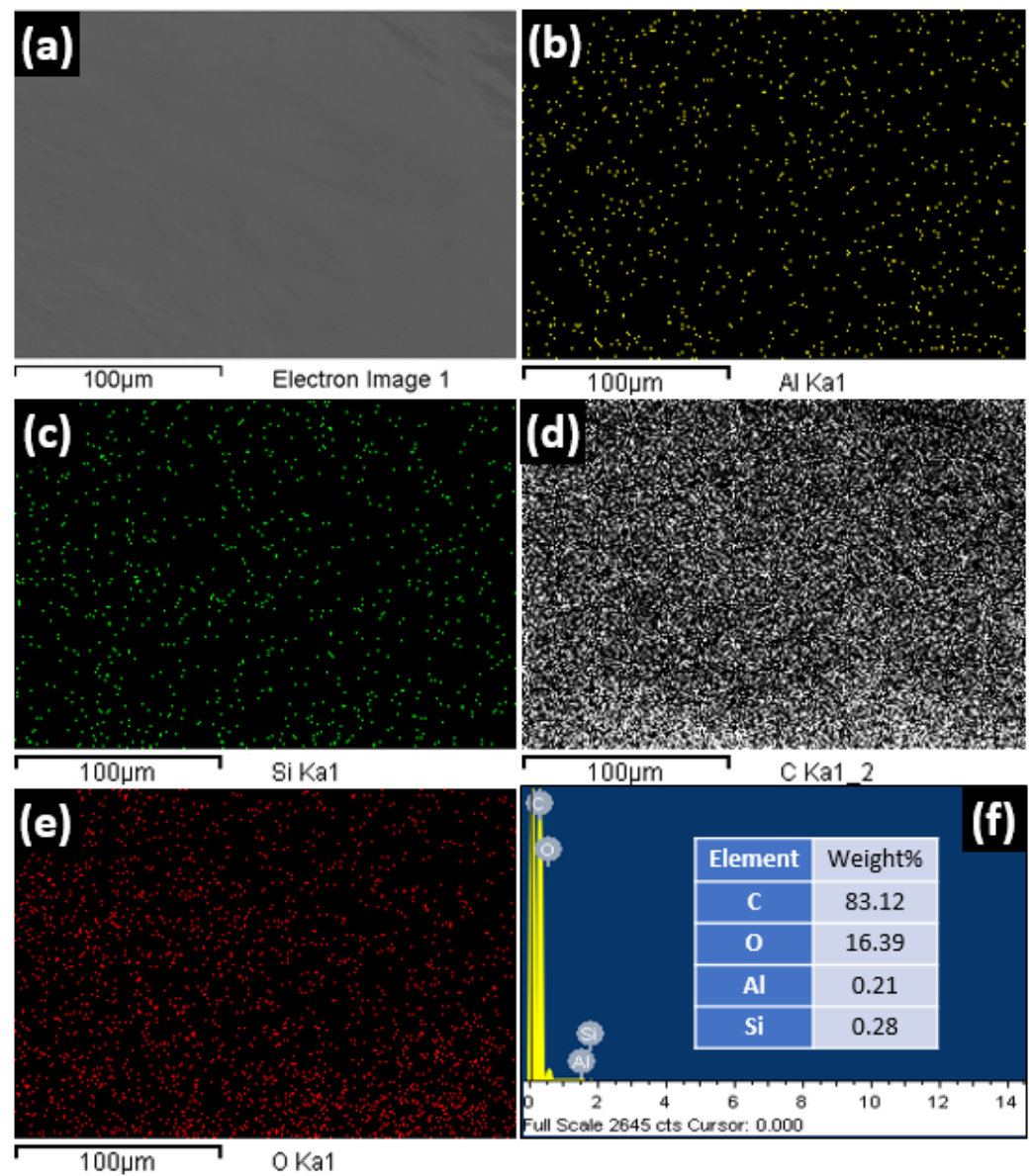


**Figure 5.** Mapping images for the highest concentration LDPE-3 sample (a) Original SEM, (b) Al distribution, (c) Si distribution, (d) Carbon distribution, (e) Oxygen distribution and (f) EDX analysis.

**Table 1.** Samples designation codes and TGA results for the LDPE and its composites.

Samples Code	Composition in wt%			Temperature (°C)		
	LDPE	Al <sub>2</sub> O <sub>3</sub>	SiC	Onset	Peak	Final
LDPE-0	100%	0%	0%	454.3	474.65	488
LDPE-1	99.8%	0.10%	0.10%	453.7	474.31	499
LDPE-2	99.5%	0.25%	0.25%	453.5	474.57	501
LDPE-3	99.0%	0.50%	0.50%	453.8	474.13	500

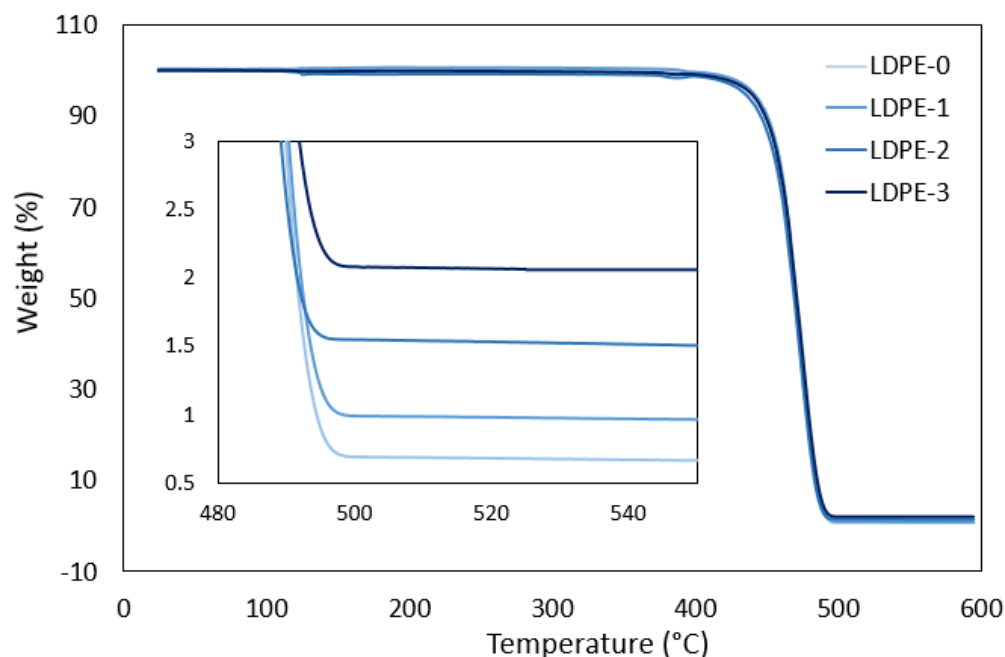


Figure 6. TGA curves for the LDPE and its composites.

The MFI of the pure LDPE is 9.41 g/10 min at the temperature of 230 °C and weight of 5 kg. The MFI decreases with increasing the hybrid filler materials, as shown in Figure 7. The decrease in MFI was reported by other researchers for the same composite [25] and could be attributed to lowering the mobility of the polymer molecule chains in the LDPE matrix [35]. Since the SiC is relatively harder and costlier than Al<sub>2</sub>O<sub>3</sub>, both reinforcements will result in better wear properties. However, the selection of Al<sub>2</sub>O<sub>3</sub> as reinforcement is made based on cost-effective selection.

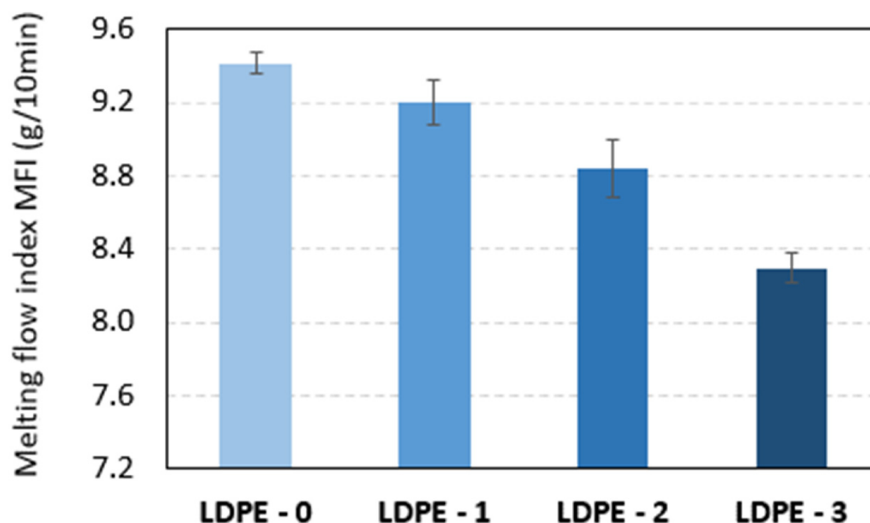


Figure 7. Melting flow index (MFI) for pure LDPE and different nanocomposite samples.

### 3.3. Mechanical Testing

In order to evaluate the mechanical properties of the fabricated nanocomposite, a series of mechanical tests were carried out as per the ASTM standards for each test as follow:

#### 3.3.1. Shore-D Hardness Test

Figure 8 shows the hardness values variation along the different fabricated nanocomposites using Shore-D type. The hardness values are slightly increased by increasing the

hybrid fillers. Although the change in the hardness values are fairly slight even for the higher amount composite (8.15%), it is in line with the slight increases in the percentage of hybrid additives. The slight improvement in the hardness can be attributed to the dislocation movement prevention as a result of imbedding those filler nanoparticles in the LDPE matrix [36]. The same strengthening mechanism can also contribute to the load bearing capacity of the nanocomposite, which reflected on the mechanical properties as clarified in the tensile section.

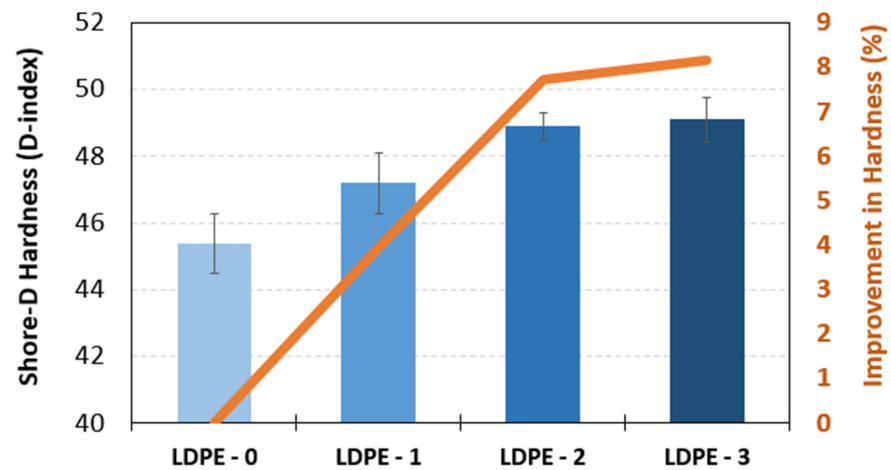


Figure 8. Shore-D hardness values for pure LDPE and different nanocomposite samples.

### 3.3.2. Tensile and Flextural Test

Silicon carbide and Alumina added to the LDPE matrix successfully improved tensile characteristics while decreasing ductility somewhat. The tensile test results are shown in Figure 9. The figure clearly shows that the composite's tensile characteristics are improved over the neat LDPE. The enhancement could be attributed to the improved dispersion of the hybrid nanofiller in the LDPE because of using more than one extrusion shot which subsequently leads to better interfacial bonding between the hybrid additives and the LDPE matrix.

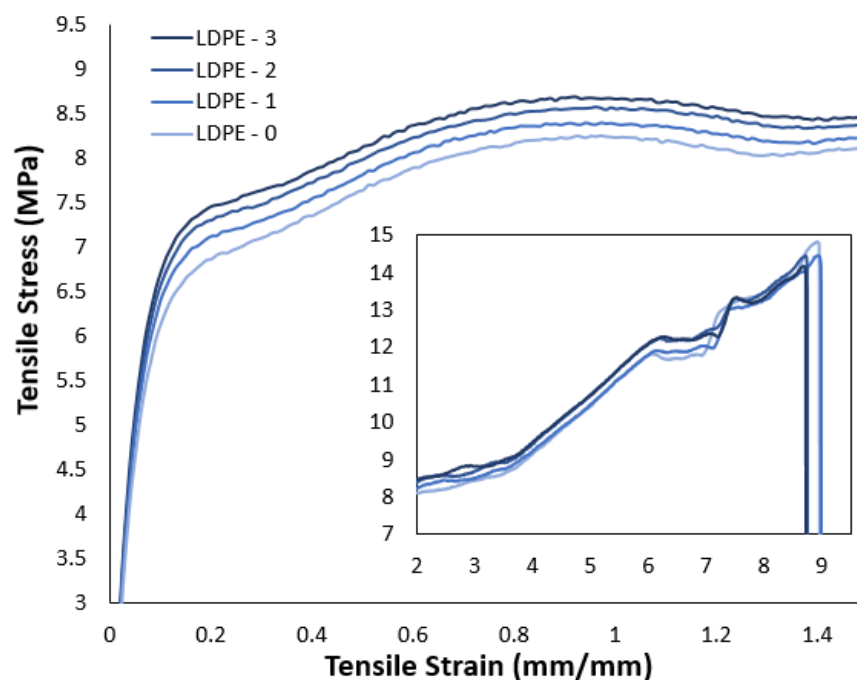
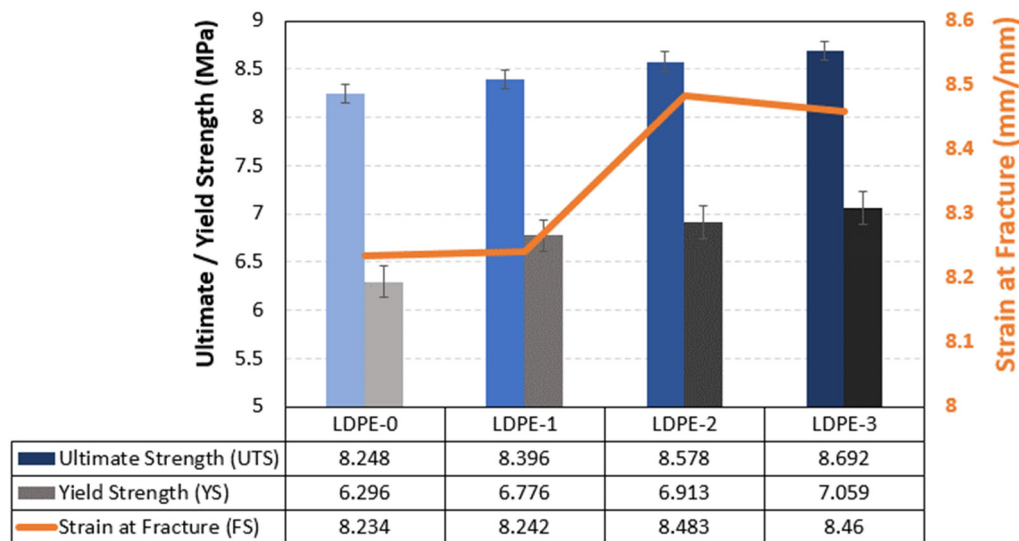


Figure 9. Typical stress–strain curves for pure LDPE and different nanocomposite samples.

The study’s findings reveal that the tensile properties of low-density polyethylene (LDPE) can be significantly improved by incorporating low fractions of aluminum oxide (Al<sub>2</sub>O<sub>3</sub>) and silicon carbide (SiC) additives. In the experiment, the neat LDPE specimens exhibited an average yield strength of 6.296 MPa and an ultimate tensile strength of 8.248 MPa. However, when the LDPE was reinforced with a combination of 0.5 wt% Al<sub>2</sub>O<sub>3</sub> and 0.5 wt% SiC, the yield strength increased to 7.059 MPa and the ultimate tensile strength rose to 8.692 MPa as represented in Figure 10. This corresponds to an enhancement of 12.12% and 5.38% in yield strength and ultimate tensile strength, respectively.



**Figure 10.** Ultimate tensile strength (UTS), yield strength (YS) and strain at fracture (FS) for pure LDPE and different nanocomposite samples.

The primary factor responsible for the observed improvement in the mechanical properties of the LDPE reinforced with hybrid ceramic nanoparticles is the increase in crystallinity within the polymer matrix. This increase in crystallinity is attributed to the incorporation of high crystalline additives, such as Al<sub>2</sub>O<sub>3</sub> and SiC, into the polymer matrix [36]. The presence of these additives promotes the formation of a more ordered and structured arrangement of polymer chains, which in turn leads to enhanced mechanical properties, including increased tensile strength and yield strength.

Flexural strength of the composites was calculated and plotted in the graph as shown in Figure 11. The figure shows that increasing the weight % of the hybrid additives has little positive effect on the flexural strength. This might be due to the incorporation of low volume fraction from the hard and stiff alumina/silicon carbide particles in the LDPE matrix. Those nanoparticles resist the deformation of the nanocomposite resulting a slight improvement in the flexural strength values. The maximum improvement in the flexural load was 19.4 % at displacement of 20 mm for LDPE with 0.5 Al<sub>2</sub>O<sub>3</sub> and 0.5 SiC.

Based on the results, LDPE reinforced with SiC/Al<sub>2</sub>O<sub>3</sub> has a higher tensile strength than base LDPE. Alumina and SiC additives increase brittleness as weight percentages increase, confirming that elongation decreases with increasing wt% of additives. According to this study, the trend of UTS and Yield strength increases when the weight % of SiC and Alumina in the matrix increases. A discrepancy between additives and matrix causes a high-stress concentration at the particle, and the matrix in that region collapses prematurely when loaded [37,38]. With a higher volume fraction, there is a substantial tendency for particle clustering, resulting in a relatively inefficient load transmission mechanism. That is the reason for using low volume fraction additives.

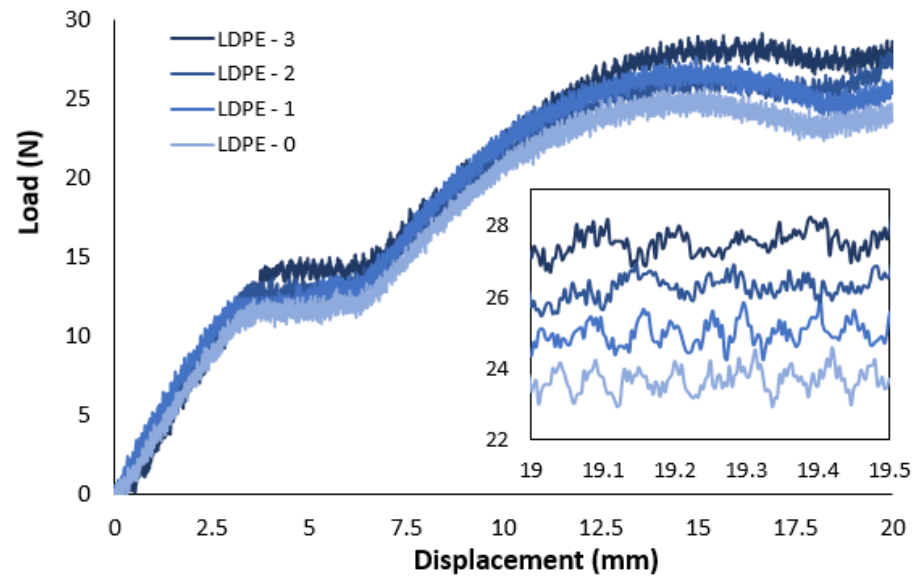


**Figure 11.** Typical Load-Displacement curves for pure LDPE and different nanocomposite samples.

### 3.4. Tribological Performance

In order to explore the impact of incorporating aluminum oxide and silicon carbide nanoparticles at various weight fractions on the tribological properties of LDPE nanocomposites, samples of the nanocomposite were subjected to frictional tests against a stainless-steel ball. The tests were conducted at a consistent linear speed of 0.4 m/s, while the applied loads ranged from 10 N to 50 N. After that, the average friction coefficient and wear mass loss were estimated. Figure 12 depicts the fluctuations in the friction coefficient in response to the change in the normal load. Notably, the incorporation of aluminum oxide and silicon carbide nanoparticles reduced the friction coefficient of the LDPE nanocomposite samples, as compared to the net LDPE, with various applied loads. The findings indicate that LDPE0.5 exhibited the lowest coefficient of friction, 0.24, which is 12.5% lower than the coefficient of friction of net LDPE (0.27) under a normal load of 10 N. The decrease in the coefficient of friction between LDPE0 and LDPE3 under other normal loads was approximately 8%.

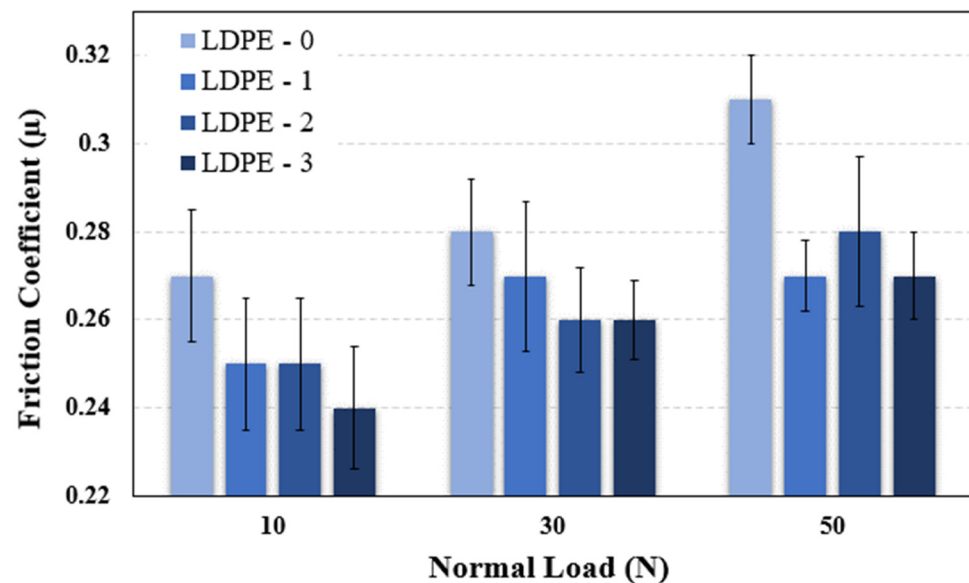


**Figure 12.** Friction coefficient of LDPE nanocomposites under different normal loads.

Additionally, Figure 12 demonstrates a gradual rise in the coefficient of friction with the increase in the normal load. This increase in the coefficient of friction can be attributed to the elevated temperature at the contact area between the surfaces in contact during the friction test [39]. The temperature rise can alter the contact area between the rubbing surfaces, thus influencing the adhesion between the tested samples and their counterparts [40].

Figure 13 demonstrates the impact of incorporating aluminum oxide and silicon carbide nanoparticles into the LDPE matrix on the wear of the nanocomposite samples during the friction experiment. The results indicate that raising these nanoparticles' weight fraction reduced the nanocomposite samples' wear. The results prove that the nanocomposite samples' wear resistance improved as the weight fraction of aluminum oxide and silicon carbide nanoparticles increased. This improvement can be attributed to the enhanced mechanical properties achieved by incorporating these nanoparticles, such as increased strength of the nanocomposite samples with higher nanoparticle concentrations. Consequently, the stronger bonding between the aluminum oxide and silicon carbide nanoparticles and LDPE matrix resulted in an enhanced load-carrying capacity, reducing the nanocomposite surfaces' degradation during the friction test. The same behavior was reported previously by other researchers [41].

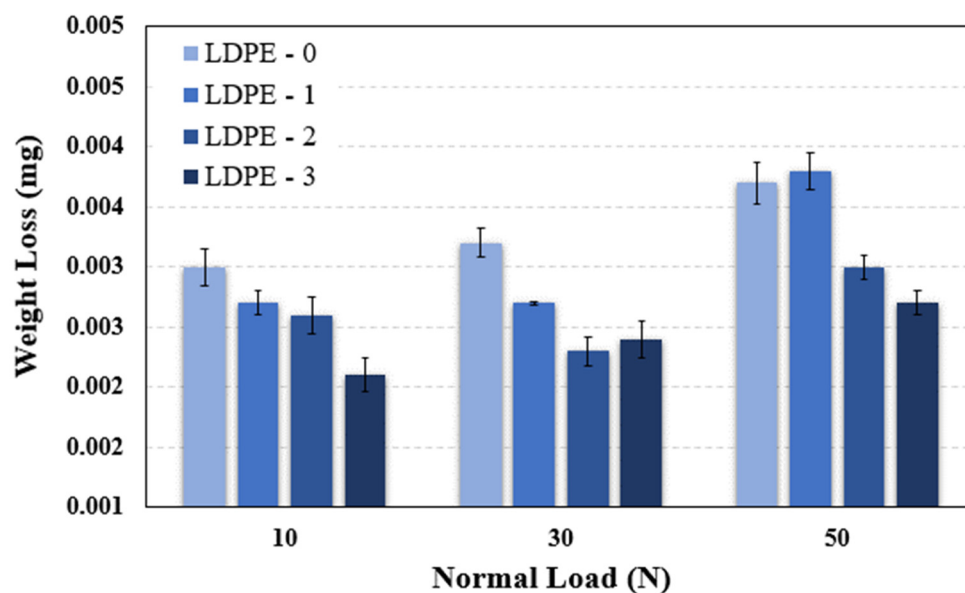


Figure 13. Wear of LDPE nanocomposites under different normal loads with a stainless-steel surface.

Additionally, the increased hardness of the LDPE nanocomposite surfaces, resulting from higher concentrations of aluminum oxide and silicon carbide, contributed to the improved wear resistance of the nanocomposite, which come in sequence with other previous work [42]. On the contrary, the weight loss of the nanocomposites increased with an increase in the normal load. This can be attributed to the rise in temperature between the rubbing surfaces, which occurs along with the increase in the normal load. The increased frictional force due to the higher normal load leads to a surface breakdown of the nanocomposite, resulting in higher weight loss.

The reduction in friction coefficient and wear can be attributed to the improved load-carrying capacity of the LDPE nanocomposite achieved by incorporating aluminum oxide and silicon carbide nanoparticles.

Measuring the contact stresses is a method used for identifying the load carrying capacity of the material. Kuminek et al. [43] sought to develop a numerical model that relate the contact stresses by the load carrying capacity of a material. They found that as the contact stresses decrease, the load carrying capacity increases. Based on that many researchers used this idea in evaluating the load carrying capacity of their developed materials. Guanchen et al. [44] claimed that the direct contact of the friction pairs happens,

and the increased interface wear would affect the load carrying capacity of the contact interface. Consequently, they developed a finite element model to identify the contact stresses generated on the surface composite structure with micro-grooves. They could find also that the increase in the strength was accompanied by a decrease in the contact stresses. From this standpoint, many researchers used the finite element models in evaluating the load carrying capacity of the material from the generated stresses during the friction process [41,45,46]. The evaluation of load-carrying capacity involved measuring the distribution of contact stress across the surface of the nanocomposite sample during the friction process [43]. A finite element model for the frictional test was created using ANSYS software using the explicit dynamics package, as illustrated in Figure 14, to simulate and analyze the frictional process and estimate the contact stresses.

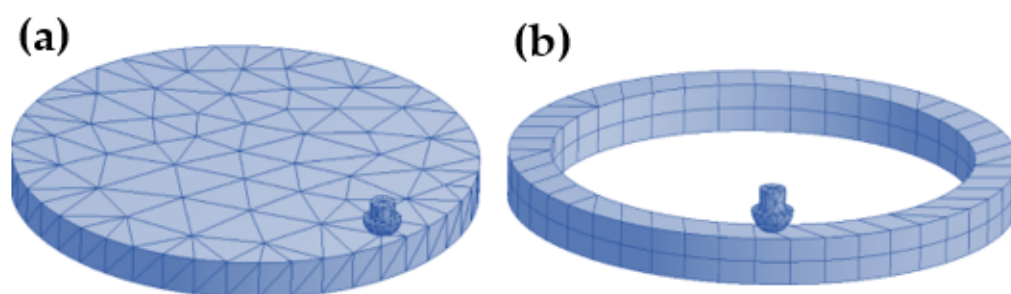


**Figure 14.** FEM of the LDPE nanocomposite sample under frictional process (a) real model, and (b) simplified model.

The LDPE nanocomposite was modeled as a circular disc with a diameter of 60 mm, as shown in Figure 14a. The disc was hollowed out to simplify the model, decrease solving time and focus on measuring the contact stresses, as shown in Figure 14b. The contact between the ball and the LDPE nanocomposite disc was defined as frictional, allowing for estimating stresses resulting from the tribological test. The automatic meshing feature of the software was used to create the mesh for the ball and the disc. The mesh consisted of hexahedral and tetrahedral elements, dividing the two parts into 263 elements and 1167 nodes. Boundary conditions were applied to the model, with the ball fixed in the X and Y directions, and a normal force of  $-50$  N was applied to the ball in the Z direction. The mechanical properties of the nanocomposite were incorporated into the ANSYS software according to the experimental findings.

The SEM images shown in Figure 15 illustrate the worn surfaces of the different LDPE composites. The configuration and characteristics of the dispersed phase clusters vary depending on the extent of polymer adhesion and its interaction with the reinforcement material. The presence of micro-voids surrounding these clusters suggests that the bond at the interface was feeble, either between polymer chains or between the polymer and additives. In Figure 15a, it can be observed that the surface of pure LDPE exhibits numerous significant delaminated aggregates and some voids, indicating degradation of the surface. This degradation is responsible for heightened wear, and the presence of aggregates rises the shear resistance, consequently leading to an increase in the measured friction coefficient. In this scenario, the principal wear mechanism is delamination. Figure 15b demonstrating that the incorporation of  $0.1 + 0.1$  of  $\text{Al}_2\text{O}_3$  and SiC into LDPE results in a reduction in the size of the dispersed phase aggregates. Furthermore, the emergence of microcracks and pores becomes evident. The prevailing wear mechanism under these circumstances is a fatigue-delamination mechanism. As the weight fraction of additive materials in LDPE increases, there is an enhancement in the uniform dispersion of reinforcement within the LDPE matrix. This improvement also leads to a decrease in the dimensions of both aggregates and particles, as illustrated in Figure 15c. Elevating the content of  $\text{Al}_2\text{O}_3$  and SiC to 0.5 wt.% resulted in heightened hardness and enhanced bonding strength within the composites. This increase in interfacial adhesion between the LDPE matrix and the additive nanoparticles promotes the efficient transfer of stresses, thereby augmenting the surface's

resistance to wear. As a result, Figure 15d reveals minimal presence of cracks and debris on the composite surface, contributing to a reduction in both wear and friction coefficient.

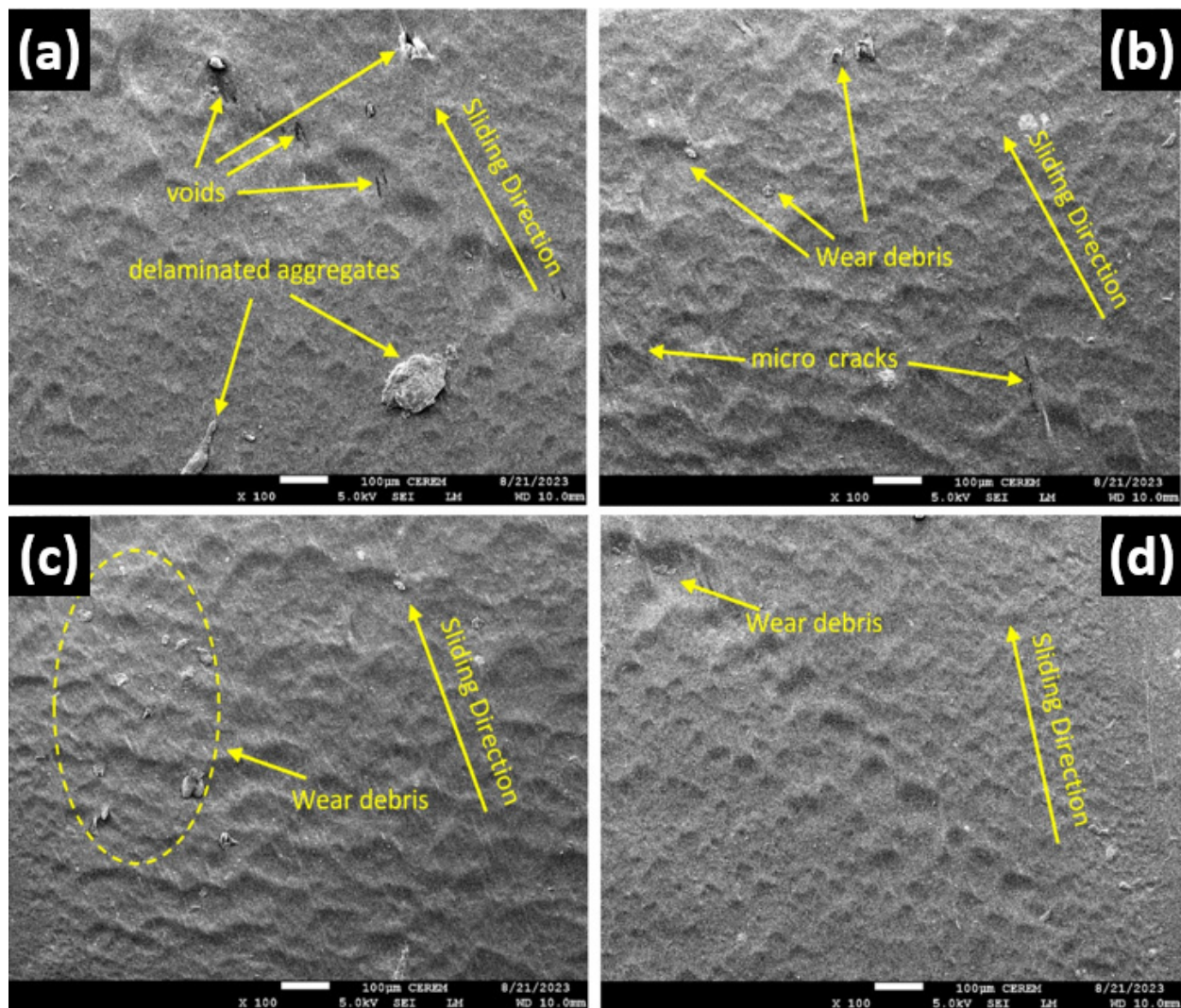


Figure 15. SEM micrographs for the wear surface (a) LDPE-0, (b) LDPE-1, (c) LDPE-2 and (d) LDPE-3.

Figure 16 presents the equivalent stress and maximum shear stress distribution on the surfaces of the LDPE nanocomposite. Figure 17 shows the variation in generated stresses on the rubbed surfaces of the nanocomposite with changing concentrations of aluminum oxide and silicon carbide nanoparticles. The results indicate a decrease in both equivalent stress and maximum shear stress, reducing the friction coefficient of the LDPE nanocomposite [41]. The finite element results are consistent with the experimental results. The decrease in the generated stresses with the enhancement in the mechanical properties led to a reduction in the wear rate.

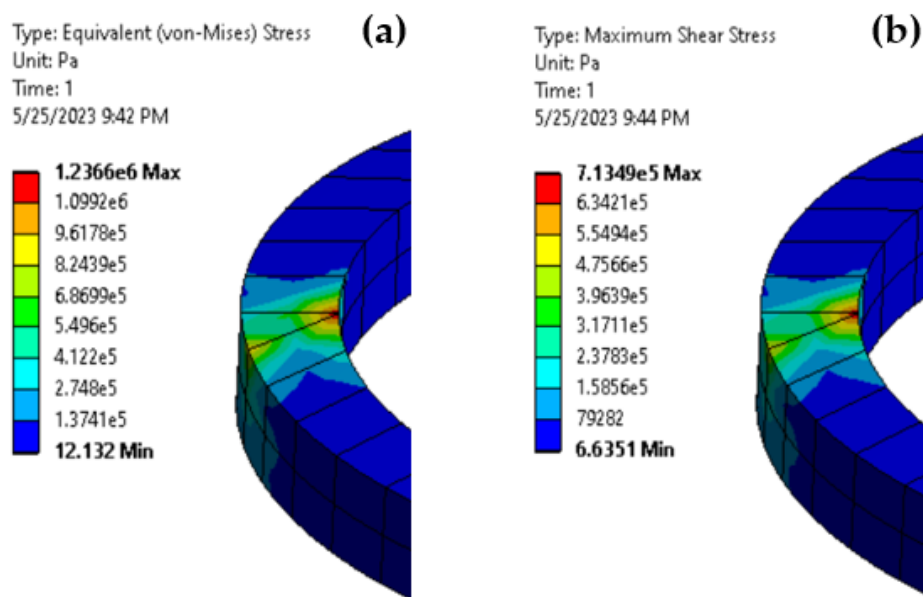


Figure 16. Stresses distribution along the LDPE nanocomposite surfaces, (a) equivalent (von-mises) stress and (b) maximum shear stress.

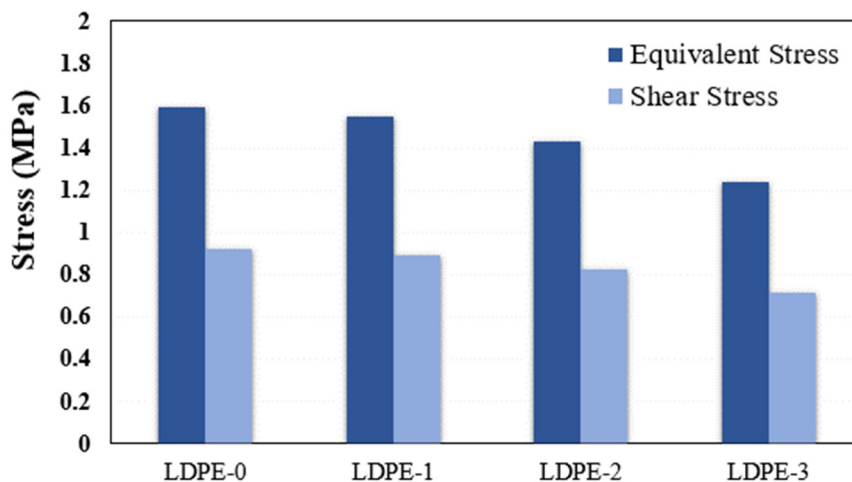


Figure 17. Equivalent von-mises and shear stress on the LDPE nanocomposite surfaces.

#### 4. Conclusions

In this study, two nanostructured oxides, particularly aluminum oxide ( $Al_2O_3$ ) and silicon carbide (SiC) nanoparticles, were employed as low fraction hybrid reinforcements for the low-density polyethylene (LDPE) matrix. The polymer/ceramic filler mixtures were homogeneously blended using a twin-screw extruder, and the nanocomposite samples were successfully fabricated via an injection molding technique. The following conclusions can be drawn from the research findings:

- Employing two rounds of extrusion shots before injection molding effectively produces homogeneous nanocomposite samples with well-dispersed low fraction additives.
- Incorporating alumina and silicon carbide nanoparticles into the LDPE matrix leads to increased tensile strength, yield strength and hardness. The study findings revealed improvements of 5.38%, 17.4% and 8.15%, respectively, for the LDPE + 0.5% $Al_2O_3$  + 0.5%SiC composite.
- The melt flow index (MFI) decreases as the hybrid filler content increases. The maximum reduction of 11.9% was observed for the LDPE + 0.5% $Al_2O_3$  + 0.5%SiC composite.

This decrease in MFI can be attributed to the reduced mobility of the polymer molecular chains within the LDPE matrix.

- The lowest coefficient of friction was recorded for the LDPE + 0.5%Al<sub>2</sub>O<sub>3</sub> + 0.5%SiC composite under a normal load of 10 N, which was approximately 12.5% lower than that of the neat LDPE, which is because the enhanced mechanical properties achieved by incorporating these nanoparticles.
- The incorporation of a low fraction of Al<sub>2</sub>O<sub>3</sub>/SiC during the fabrication of composites increased the load-carrying capacity, as evidenced by the finite element analysis results. Consequently, the enhanced mechanical properties led to reduced stress generation and a lower wear rate.
- The application of aluminum oxide (Al<sub>2</sub>O<sub>3</sub>) and silicon carbide (SiC) nanoparticles as hybrid reinforcements in low-density polyethylene (LDPE) matrix offers the potential for lightweight materials with improved mechanical properties and enhanced tribological performance. These nanocomposites could find applications in various industries where strength, hardness and reduced friction are desired, opening up possibilities for more efficient and durable products.

**Author Contributions:** Conceptualization, H.S.A. and I.A.A.; methodology, H.S.A., M.O.A. and J.A.M.; software, A.F., M.B.E. and H.S.A.; validation, I.A.A., A.F., M.O.A., J.A.M., M.B.E. and H.S.A.; formal analysis, I.A.A., A.F., M.O.A., J.A.M., M.B.E., S.A.R. and H.S.A.; investigation, I.A.A., A.F., M.O.A., J.A.M. and H.S.A.; data curation, I.A.A., A.F., M.O.A., J.A.M. and H.S.A.; writing—original draft preparation, I.A.A., A.F., M.O.A., J.A.M. and H.S.A.; writing—review and editing, H.S.A.; visualization, I.A.A., A.F., M.O.A., J.A.M., M.B.E., S.A.R. and H.S.A.; supervision H.S.A.; project administration, H.S.A.; funding acquisition, H.S.A. All authors have read and agreed to the published version of the manuscript.

**Funding:** This research was funded by Deputyship for Research and Innovation, Ministry of Education in Saudi Arabia for funding this research work through the project no. (IFKSUOR3–074–2).

**Institutional Review Board Statement:** Not applicable.

**Informed Consent Statement:** Not applicable.

**Data Availability Statement:** Data used to support the findings of this study are available from the corresponding author upon request.

**Acknowledgments:** The authors extend their appreciation to the Deputyship for Research and Innovation, Ministry of Education in Saudi Arabia for funding this research work through the project no. (IFKSUOR3–074–2).

**Conflicts of Interest:** The authors declare no conflict of interest.

## References

1. Mirizzi, L.; D'Arienzo, M.; Nisticò, R.; Fredi, G.; Diré, S.; Callone, E.; Dorigato, A.; Giannini, L.; Guerra, S.; Mostoni, S.; et al. Al<sub>2</sub>O<sub>3</sub> decorated with polyhedral silsesquioxane units: An unconventional filler system for upgrading thermal conductivity and mechanical properties of rubber composites. *Compos. Sci. Technol.* **2023**, *236*, 109977. [[CrossRef](#)]
2. Fouly, A.; Almotairy, S.M.; Aijaz, M.O.; Alharbi, H.F.; Abdo, H.S. Balanced Mechanical and Tribological Performance of High-Frequency-Sintered Al-SiC Achieved via Innovative Milling Route—Experimental and Theoretical Study. *Crystals* **2021**, *11*, 700. [[CrossRef](#)]
3. Ahamed, T.; Brown, S.P.; Salehi, M. Investigate the role of biofilm and water chemistry on lead deposition onto and release from polyethylene: An implication for potable water pipes. *J. Hazard. Mater.* **2020**, *400*, 123253. [[CrossRef](#)]
4. Avcioglu, S. LDPE matrix composites reinforced with dysprosium-boron containing compounds for radiation shielding applications. *J. Alloys Compd.* **2022**, *927*, 166900. [[CrossRef](#)]
5. Videira-Quintela, D.; Guillén, F.; Martín, O.; Montalvo, G. Antibacterial LDPE films for food packaging application filled with metal-fumed silica dual-side fillers. *Food Packag. Shelf Life* **2022**, *31*, 100772. [[CrossRef](#)]
6. Polanský, R.; Kadlec, P.; Slepíčka, P.; Kolská, Z.; Švorčík, V. Testing the applicability of LDPE/HNT composites for cable core insulation. *Polym. Test.* **2019**, *78*, 105993. [[CrossRef](#)]
7. Benabid, F.Z.; Mallem, O.K.; Zouai, F.; Cagiao, M.E.; Benachour, D. Effect of the Mechanical Treatment of Alumina on Thermal, Morphological and Dielectric Properties of LDPE/Al<sub>2</sub>O<sub>3</sub> Composites. *South African J. Chem.* **2018**, *71*, 150–154. [[CrossRef](#)]

8. Chee, C.Y.; Song, N.L.; Abdullah, L.C.; Choong, T.S.Y.; Ibrahim, A.; Chantara, T.R. Characterization of mechanical properties: Low-density polyethylene nanocomposite using nanoalumina particle as filler. *J. Nanomater.* **2012**, *2012*, 118. [[CrossRef](#)]
9. Wu, Y.; Dong, C.; Yuan, C.; Bai, X.; Zhang, L.; Tian, Y. MWCNTs filled high-density polyethylene composites to improve tribological performance. *Wear* **2021**, *477*, 203776. [[CrossRef](#)]
10. Brostow, W.; Hagg Lobland, H.E.; Hnatchuk, N.; Perez, J.M. Improvement of Scratch and Wear Resistance of Polymers by Fillers Including Nanofillers. *Nanomaterials* **2017**, *7*, 66. [[CrossRef](#)]
11. Panin, S.V.; Kornienko, L.A.; Alexenko, V.O.; Buslovich, D.G.; Bochkareva, S.A.; Lyukshin, B.A. Increasing Wear Resistance of UHMWPE by Loading Enforcing Carbon Fibers: Effect of Irreversible and Elastic Deformation, Friction Heating, and Filler Size. *Materials* **2020**, *13*, 338. [[CrossRef](#)]
12. Kayode Aliyu, I.; Abdul Samad, M.; Al-Qutub, A.M. Friction and wear behavior of ultra-high molecular weight polyethylene/graphene nanoplatelets nanocomposite coatings at elevated temperatures. *J. Eng. Tribol.* **2021**, *236*, 1782–1788. [[CrossRef](#)]
13. Zhang, L.; Qi, H.; Li, G.; Wang, D.; Wang, T.; Wang, Q.; Zhang, G. Significantly enhanced wear resistance of PEEK by simply filling with modified graphitic carbon nitride. *Mater. Des.* **2017**, *129*, 192–200. [[CrossRef](#)]
14. Fouly, A.; Alnaser, I.A.; Assaifan, A.K.; Abdo, H.S. Evaluating the Performance of 3D-Printed PLA Reinforced with Date Pit Particles for Its Suitability as an Acetabular Liner in Artificial Hip Joints. *Polymers* **2022**, *14*, 3321. [[CrossRef](#)]
15. Pelto, J.; Verho, T.; Ronkainen, H.; Kaunisto, K.; Metsäjoki, J.; Seitsonen, J.; Karttunen, M. Matrix morphology and the particle dispersion in HDPE nanocomposites with enhanced wear resistance. *Polym. Test.* **2019**, *77*, 105897. [[CrossRef](#)]
16. Liu, T.; Li, B.; Lively, B.; Eyler, A.; Zhong, W.H. Enhanced wear resistance of high-density polyethylene composites reinforced by organosilane-graphitic nanoplatelets. *Wear* **2014**, *309*, 43–51. [[CrossRef](#)]
17. Burris, D.L.; Boesl, B.; Bourne, G.R.; Sawyer, W.G.; Burris, D.L.; Boesl, B.; Bourne, G.R.; Sawyer, W.G. Polymeric Nanocomposites for Tribological Applications. *Macromol. Mater. Eng.* **2007**, *292*, 387–402. [[CrossRef](#)]
18. Burris, D.L.; Zhao, S.; Duncan, R.; Lowitz, J.; Perry, S.S.; Schadler, L.S.; Sawyer, W.G. A route to wear resistant PTFE via trace loadings of functionalized nanofillers. *Wear* **2009**, *267*, 653–660. [[CrossRef](#)]
19. Pelto, J.; Heino, V.; Karttunen, M.; Rytöluoto, I.; Ronkainen, H. Tribological performance of high density polyethylene (HDPE) composites with low nanofiller loading. *Wear* **2020**, *460–461*, 203451. [[CrossRef](#)]
20. Noorunnisa Khanam, P.; Al-Maadeed, M.A.; Mrlik, M. Improved flexible, controlled dielectric constant material from recycled LDPE polymer composites. *J. Mater. Sci. Mater. Electron.* **2016**, *27*, 8848–8855. [[CrossRef](#)]
21. Deepak, D.; Goyal, N.; Rana, P.; Gupta, V.K. Effect of varying reinforcement content on the mechanical properties of hemp-recycled HDPE composites. *Mater. Today Proc.* **2019**, *18*, 5286–5291. [[CrossRef](#)]
22. Samad, U.A.; Alam, M.A.; Abdo, H.S.; Anis, A.; Al-Zahrani, S.M. Synergistic Effect of Nanoparticles: Enhanced Mechanical and Corrosion Protection Properties of Epoxy Coatings Incorporated with SiO<sub>2</sub> and ZrO<sub>2</sub>. *Polymers* **2023**, *15*, 3100. [[CrossRef](#)] [[PubMed](#)]
23. Abdo, H.S.; Seikh, A.H. Correlation of Microstructure with Compression Behaviour of Al5083/ZrC Nanocomposites Fabricated Through Spark Plasma Sintering. *Trans. Indian Inst. Met.* **2022**, *75*, 2273–2280. [[CrossRef](#)]
24. Abdo, H.S.; Samad, U.A.; Abdo, M.S.; Alkhamash, H.I.; Aijaz, M.O. Electrochemical Behavior of Inductively Sintered Al/TiO<sub>2</sub> Nanocomposites Reinforced by Electrospun Ceramic Nanofibers. *Polymers* **2021**, *13*, 4319. [[CrossRef](#)]
25. Bedi, P.; Singh, R.; Ahuja, I.P.S. Effect of SiC/Al<sub>2</sub>O<sub>3</sub> particle size reinforcement in recycled LDPE matrix on mechanical properties of FDM feed stock filament. *Virtual Phys. Prototyp.* **2018**, *13*, 246–254. [[CrossRef](#)]
26. De Abreu Ferreira Cardoso, B.F.; Ramos, F.J.H.T.V.; Da Silveira, P.H.P.M.; De Oliveira, A.G.B.A.M.; Da Silva Figueiredo, A.B.H.; Gomes, A.V.; Da Veiga, V.F. Mechanical and ballistc characterization of high-density polyethylene composites reinforced with alumina and silicon carbide particles. *J. Met. Mater. Miner.* **2022**, *32*, 42–49. [[CrossRef](#)]
27. Hayun, S.; Paris, V.; Mitrani, R.; Kalabukhov, S.; Dariel, M.P.; Zaretsky, E.; Frage, N. Microstructure and mechanical properties of silicon carbide processed by Spark Plasma Sintering (SPS). *Ceram. Int.* **2012**, *38*, 6335–6340. [[CrossRef](#)]
28. Naga, S.M.; El-Maghraby, H.F.; Elgamhoudy, M.; Saleh, M.A. Characterization and origin of failure of SiC/ZTA composites. *Int. J. Refract. Met. Hard Mater.* **2018**, *73*, 53–57. [[CrossRef](#)]
29. ASTM D1238-13; Standard Test Method for Melt Flow Rates of Thermoplastics by Extrusion Plastometer. ASTM International: West Conshohocken, PA, USA, 2013.
30. ASTM D2240-15; Standard Test Method for Rubber Property—Durometer Hardness. ASTM International: West Conshohocken, PA, USA, 2015, 2015. [[CrossRef](#)]
31. ASTM D790-17; Standard Test Methods for Flexural Properties of Unreinforced and Reinforced Plastics and Electrical Insulating Materials. ASTM International: West Conshohocken, PA, USA, 2017. [[CrossRef](#)]
32. ASTM D638-22; Standard Test Method for Tensile Properties of Plastics. ASTM International, 2022. [[CrossRef](#)]
33. ASTM G99-17; Standard Test Method for Wear Testing with a Pin-on-Disk Apparatus. ASTM International: West Conshohocken, PA, USA, 2017. [[CrossRef](#)]
34. Mallakpour, S.; Dinari, M. Enhancement in thermal properties of poly(vinyl alcohol) nanocomposites reinforced with Al<sub>2</sub>O<sub>3</sub> nanoparticles. *J. Reinf. Plast. Compos.* **2013**, *32*, 217–224. [[CrossRef](#)]
35. Junaedi, H.; Baig, M.; Dawood, A.; Albahkali, E.; Almajid, A. Mechanical and Physical Properties of Short Carbon Fiber and Nanofiller-Reinforced Polypropylene Hybrid Nanocomposites. *Polymers* **2020**, *12*, 2851. [[CrossRef](#)]

36. Khamaj, A.; Farouk, W.M.; Shewakh, W.M.; Abu-Oqail, A.M.I.; Wagih, A.; Abu-Okail, M. Effect of lattice structure evolution on the thermal and mechanical properties of Cu–Al<sub>2</sub>O<sub>3</sub>/GNPs nanocomposites. *Ceram. Int.* **2021**, *47*, 16511–16520. [[CrossRef](#)]
37. Dhabale, R.; Jatti, V.S. A bio-material: Mechanical behaviour of LDPE-Al<sub>2</sub>O<sub>3</sub>-TiO<sub>2</sub>. *IOP Conf. Ser. Mater. Sci. Eng.* **2016**, *149*, 012043. [[CrossRef](#)]
38. Padmanabhan, M.; Thokal, M. Comparison of Mechanical Properties of Al<sub>2</sub>O<sub>3</sub> And Low Density Polyethylene (LDPE). *Int. J. Eng. Res.* **2013**, *3*, 224–227.
39. Chang, L.; Zhang, Z.; Zhang, H.; Friedrich, K. Effect of nanoparticles on the tribological behaviour of short carbon fibre reinforced poly(etherimide) composites. *Tribol. Int.* **2005**, *38*, 966–973. [[CrossRef](#)]
40. Khun, N.W.; Zhang, H.; Lim, L.H.; Yue, C.Y.; Hu, X.; Yang, J. Tribological properties of short carbon fibers reinforced epoxy composites. *Friction* **2014**, *2*, 226–239. [[CrossRef](#)]
41. Fouly, A.; Alkalla, M.G. Effect of low nanosized alumina loading fraction on the physicochemical and tribological behavior of epoxy. *Tribol. Int.* **2020**, *152*, 106550. [[CrossRef](#)]
42. Campos-Sanabria, V.; Hernández-Sierra, M.T.; Bravo-Sánchez, M.G.; Aguilera-Camacho, L.D.; García-Miranda, J.S.; Moreno, K.J. Tribological and mechanical characterization of PMMA/HAp nanocomposites obtained by free-radical polymerization. *MRS Adv.* **2018**, *3*, 3763–3768. [[CrossRef](#)]
43. Kuminek, T.; Aniołek, K.; Młyńczak, J. A numerical analysis of the contact stress distribution and physical modelling of abrasive wear in the tram wheel-frog system. *Wear* **2015**, *328–329*, 177–185. [[CrossRef](#)]
44. Lu, G.; Shi, X.; Zhang, J.; Zhou, H.; Xue, Y.; Ibrahim, A.M.M. Effects of surface composite structure with micro-grooves and Sn-Ag-Cu on reducing friction and wear of Ni3Al alloys. *Surf. Coatings Technol.* **2020**, *387*, 125540. [[CrossRef](#)]
45. Alnaser, I.A.; Abdo, H.S.; Abdo, M.S.; Alkalla, M.; Fouly, A. Effect of Synthesized Titanium Dioxide Nanofibers Weight Fraction on the Tribological Characteristics of Magnesium Nanocomposites Used in Biomedical Applications. *Nanomaterials* **2023**, *13*, 294. [[CrossRef](#)]
46. Ibrahim, A.M.M.; Shi, X.; Zhang, A.; Yang, K.; Zhai, W. Tribological Characteristics of NiAl Matrix Composites with 1.5 wt% Graphene at Elevated Temperatures: An Experimental and Theoretical Study. *Tribol. Trans.* **2015**, *58*, 1076–1083. [[CrossRef](#)]

**Disclaimer/Publisher’s Note:** The statements, opinions and data contained in all publications are solely those of the individual author(s) and contributor(s) and not of MDPI and/or the editor(s). MDPI and/or the editor(s) disclaim responsibility for any injury to people or property resulting from any ideas, methods, instructions or products referred to in the content.